DOI: 10.1002/((please add manuscript number))

Article type: Communication

Super moisture-absorbent gels for all-weather atmospheric water harvesting

*Fei Zhao, Xingyi Zhou, Yi Liu, Ye Shi, Yafei Dai and Guihua Yu**

Dr. F. Zhao, X. Zhou, Dr. Y. Shi Prof, G. Yu

Materials Science and Engineering Program and Department of Mechanical Engineering, The University of Texas at Austin, TX, 78712, USA.

E-mail: ghyu@austin.utexas.edu

Y. Liu, Prof. Y. Dai

School of Physics Science & Technology and Jiangsu Key Laboratory for NSLSCS, Nanjing Normal University, Nanjing 210023, China.

Prof. Y. F. Dai

Hefei National Laboratory for Physical Sciences at Microscale, University of Science and Technology of China, Hefei, Anhui 230026, China.

Keywords: hydrogel, solar energy, moisture absorbing, water harvesting

Atmospheric water harvesting—producing fresh water via collecting moisture from air—enables sustainable water delivery without geographical and hydrologic limitations. However, the fundamental design principle to prepare materials that can convert the water vapor in the air to collectible liquid water is still mostly unknown. Here, we show a super moisture-absorbent gel, which is composed of hygroscopic polypyrrole chloride penetrating in hydrophilicity switchable polymeric network of poly N-isopropylacrylamide. Based on such design, a high-efficiency water production by atmospheric water harvesting has been achieved in a broad range of relative humidity. The synergistic effect enabled by the molecular level integration of hygroscopic and hydrophilicity-switchable polymers in a network architecture presents controllable interaction between the gel and water molecules, simultaneously realizing efficient vapor capturing, in-situ water liquefaction, high-density water storage and fast water releasing under different weather conditions. Being an effective method to regulate migration of water molecules, such design represents a novel strategy to improve the atmospheric water harvesting, and it is also fundamental to other water management systems for environmental cooling, surficial moisturizing and beyond.

A recent report by the United Nations' Intergovernmental Panel on Climate Change states that there are 3.2 billion people around the world suffering from water shortage because of the absence of water sources such as a river, lake, and groundwater in their living areas.[1] Such dire warning has motivated the research field of a new water resource — atmospheric water, which provides ca. 50,000 km^3 of water regardless of the geographical (and/or hydrologic) conditions.[2] The state-of-the-art of atmospheric water harvesting (AWH) material has demonstrated the possibility of directly collecting liquid water from air with the assistance of water condensation at ultra-high relative humidity (RH = 100 %, e.g. fog capture and dew collection).[3-8] Due to the dependence of RH on the temperature of the air, such a process requires either periodic temperature drop or artificial cooling systems to raise the RH to be supersaturated.[9] A recent report presents an AWH material functioning at low RH levels down to 20 % to harvest moisture (water vapor) from air, enabling the moisture as a promising water source for potential next-generation AWH systems.[10] In view of the seasonal and climatic variation, the RH of the droughty region (such as the Namib Desert) varies between 30 % to 90 % for most of the years.[3,11] Since

such modest RH (at given temperature and air pressure) indicates a relatively large water reservoir in the air, the highly efficient AWH toward this "rich ore" of water, which, however, remains elusive, is vital to both fundamental research and practical applications. In this context, hygroscopic materials based on surface water adsorption, such as molecular sieves, silica gels, and polymeric desiccants, can serve as the moisture absorber over a wide range of RH.[12–14] However, the hygroscopic materials designed for moisture capturing exhibit strong interaction with water that significantly hinders the water releasing, blunting their opportunity to be used as atmospheric water harvesters.[15,16]

In line with the design of super water-absorbent gels, which are capable of absorbing tens of times its own weight in liquid water,[17, 18] we present here a super moisture-absorbent gel (SMAG) that synergistically combines the moisture-absorbing hygroscopic polymer with the water-storing hydrophilic gel, which substantially outperforms other AWH materials. We demonstrate a rationally designed hybrid gel that integrates the hygroscopic chloride-doped polypyrrole (PPy-Cl) and the poly(N-isopropylacrylamide) (poly-NIPAM) with switchable hydrophilicity.[19–21] Such a SMAG realizes the polymeric-network-enabled moisture capturing, rather than active-surface-based vapor adsorption as in other AWH materials, and hence exhibits highly efficient AWH in broad humidity range. Moreover, to explore the potential application, we further demonstrate the outdoor experiments by a scalable SMAG prototype with low-cost accessories to simulate the AWH in the natural environment.

The critical steps of SMAG-based AWH are (*I*) water capturing and (*II*) water releasing. As shown in Figure 1a, the water molecules can be adsorbed, liquefied on the surface of SMAG, which is enabled by hygroscopic PPy-Cl, and then diffuse into its polymeric network matrix, achieving the water capturing from moist air. Such a process can induce the swelling of SMAG. Subsequently, the water is released, which is enabled by a shrinking of swollen SMAG based on thermal-responsive hydrophilicity switching of the polymer network (in hydrophilicity-switchable poly-NIPAM), realizes a rapid delivery of water. Moreover, enabling a cyclic AWH (Figure 1b), the dehydrated SMAG is reusable, presenting an optimized daily water collection of ca. 52.8 L and 19.2 L per kilogram of the corresponding xerogel at environmental RH of 90 % and 60 %, respectively (See Experimental Section for details). The mechanism of such AWH is revealed by both experimental and theoretical investigations. In addition, the practical application of SMAG is demonstrated by both in-lab and outdoor experiments (*Vide infra*).

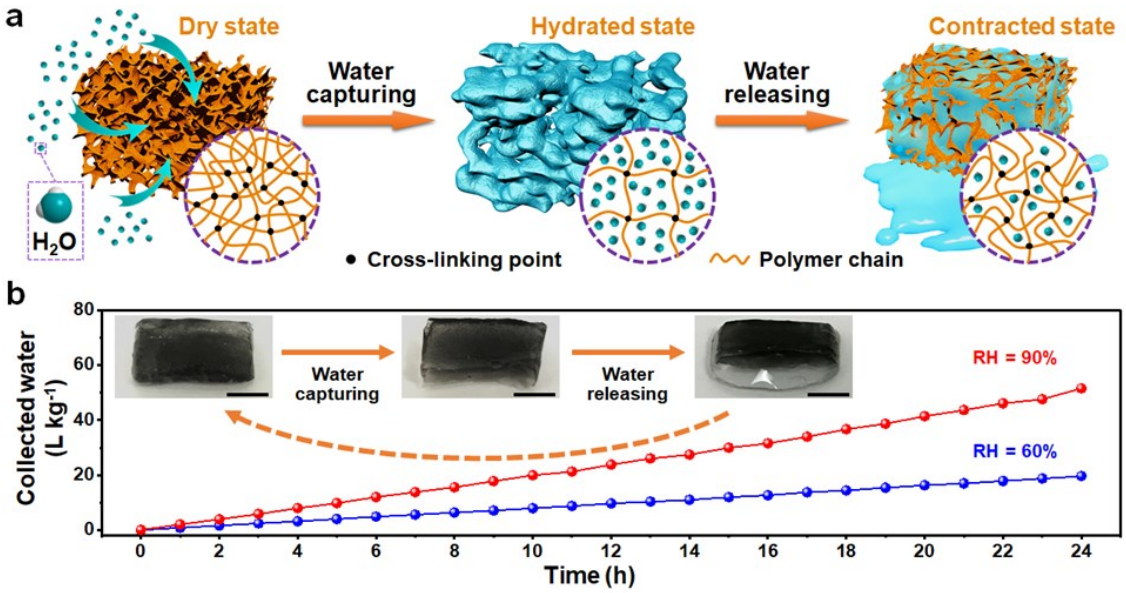

Figure 1. Atmospheric water harvesting (AWH) based on super moisture-absorbent gel (SMAG). a) Schematic illustration of the AWH process. The water molecules are captured by SMAG and liquefied under room temperature (enabled by hygroscopic chloride-doped polypyrrole). The liquid water is absorbed by polymer network matrix of SMAG, realizing the swelling in moist air. Upon exposure to heat, the contained water is released via the thermal-responsive hydrophilicity switching (from hydrophilic to hydrophobic in poly-NIPAM). b) Water production from 24 h AWH at different RH levels. Insets of b: photographs of SMAGs during typical AWH cycles (50 min for water capturing and 10 min for water releasing), with scale bars of 1 cm.

The SMAGs are prepared by the gelation of N-isopropylacrylamide (NIPAM) in a polypyrrole chloride (PPy-Cl) aqueous dispersion upon addition of N', N'-methylene bisacrylamide and ammonium persulfate as crosslinker and initiator, respectively (See Materials and Methods for details). The obtained SMAG consists of a framework of poly-NIPAM (Figure 2a), which enlarges the interfacial area of gel/air and serves as a water pathway during the water release. The hydrophilic PPy-Cl facilitates its thorough mixing with the NIPAM monomers to form an interpenetrating network after gelation.[22] The microstructure of the SMAG is characterized by scanning electron microscope (SEM), as shown in Figure 2b. Evenly distributed pores with width from several to tens of microns can be observed, serving as micron channels for water releasing. Additionally, the surface of the wall contains embedded PPy-Cl nanoparticles rather than the free-standing sphere-like pure PPy-Cl (inset of Figure 2b) or smooth surface of the pure poly-NIPAM gel (Figure S1, Supporting Information), indicating the successful integration of PPy-Cl nanoparticles into the poly-NIPAM framework.

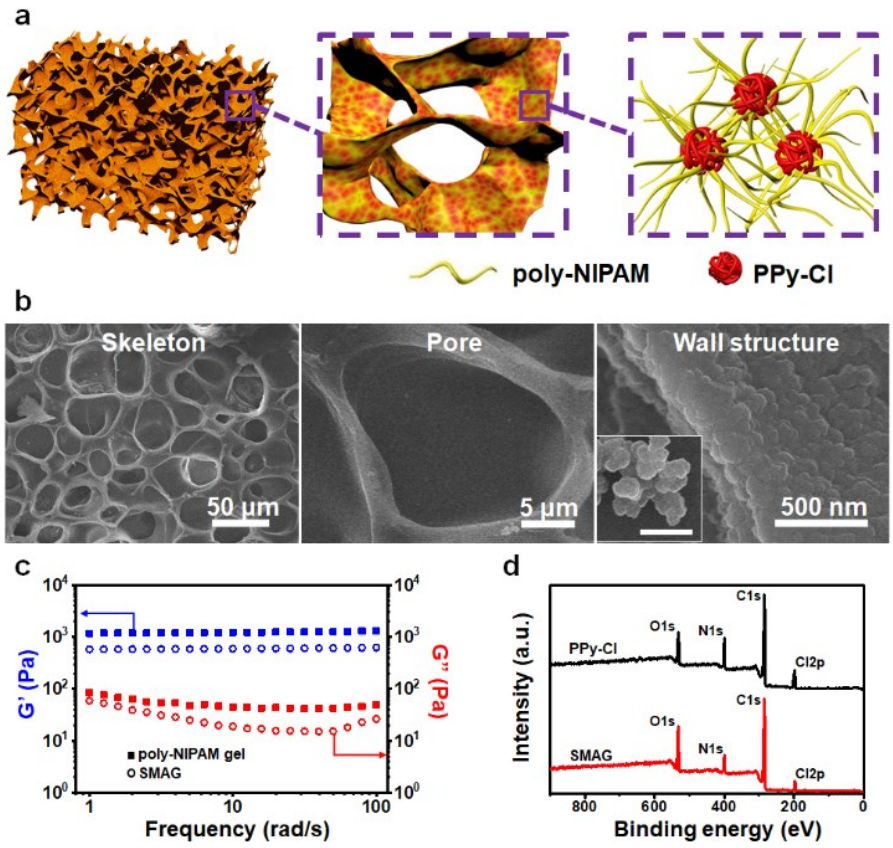

Figure 2. Characterization of the SMAG. a) Schematic of the skeleton, porous structure and an interpenetrating network of poly-NIPAM and PPy-Cl clusters; b) SEM images of a dried SMAG in different magnification, showing the porous structure, which enhances the interaction between moisture and SMAG during the adsorbing process. The rough surface of the wall structure evidences the inlay of PPy-Cl clusters in the poly-NIPAM matrix. The morphology comparison of pure PPy-Cl (inset of b with scale bar: 500 nm) and the wall structure of the SMAG further confirms the interpenetration of PPy-Cl clusters and poly-NIPAM matrix. c) Dynamic mechanical analysis, including storage modulus (G') and loss modulus (G"), demonstrates the interpenetration of PPy-Cl and poly-NIPAM in the SMAG. d) XPS of PPy-Cl and the SMAG confirm the retained chlorine dopant in obtained SMAG after purification process.

Since polymeric hydrogels are viscoelastic materials, the introduction of additive into their skeletons may alter the mechanical properties.[23] For example, the amount of energy stored in the gel system and dissipated under the oscillatory stress is indicated by the storage modulus (G') and

the loss modulus (G"), respectively. The G' and G" values of the SMAG and a pure poly-NIPAM gel are shown in Figure 2c. The dynamic frequency sweep experiments of both gels show a broad linear viscoelastic region. The value of storage modulus G' is higher than that of the loss modulus G" in both cases, confirming the formation of their cross-linked polymeric skeletons. The lower G' value of the SMAG indicates fewer cross-linking points relative to the poly-NIPAM gel, while the lower G" value of the SMAG reveals a substantial restriction of the slippage between polymer chains (also see detailed discussion in Figure S2, Supporting Information).[24] These results demonstrate substantial evidence for the insertion of the poly-NIPAM chains into the PPy-Cl clusters, leading to an interpenetrating polymeric structure of the two polymers. Moreover, this network enables a synergistic effect of hygroscopicity and hydrophilicity for efficient water capturing, which will be discussed later.

The chemical composition of the SMAG is revealed by the X-ray photoelectron spectroscopy (XPS). In Figure 2d, the peaks located at 530, 400, 285 and 200 eV can be assigned to the oxygen (O), nitrogen (N), carbon (C) and chloride (Cl).[25,26] The elemental analysis reveals an N/Cl atomic ratio of ca. 0.47 in PPy-Cl, indicating a high ratio of the dopant. In addition, the high-resolution spectra of each element further evidence that the Cl is bonded to the PPy chain and this doped state are retained in the SMAGs (Figure S3, Supporting Information). Moreover, the SMAG is also characterized by Fourier-Transform infrared (FTIR, Figure S4, Supporting Information) spectra and thermogravimetric analysis (TGA, Figure S5, Supporting Information), in which the results are in agreement with the data from XPS analysis.

The moisture absorption was investigated at various RH to assess the AWH based on SMAGs systematically. As shown by the kinetic data (**Figure 3**a), the saturated water content (hourly change lower than 1 %) are 6.7, 3.4 and 0.7 g per gram of corresponding dried SMAG (i.e. g g^{-1}) at environmental RH of 90 %, 60 % and 30 %, respectively (see Figure S6 for the influence of temperature, Supporting Information). It only takes ca. 100, 120 and 180 min for the SMAGs to be sufficiently hydrated by capturing water from air at RH of 90 %, 60 % and 30 %, respectively (Figure S7, Supporting Information). Such water capturing kinetic is almost insensitive to the environmental temperature and substrates (Figure S8, Supporting Information), while there is visible swelling (inset of Figure 3a) after hydration and the water capturing kinetics is slightly changed with the thickness of SMAG (Figure S9, Supporting Information). These results indicate that current water capturing process may feature a unique mechanism beyond previously reported moisture adsorption based solely on the ultra-large specific surface area[27-29] or dropwise condensation enabled by unique nanostructures.[4,7,30] Since the PPy-Cl exhibits hygroscopicity (Figure S10, Supporting Information), it should be the functional component boosting the water capturing of SMAG. Moreover, molecular dynamics (MD) simulation is carried out to elucidate the moisture absorbing process (See Supporting Methods for details) to further study the moisture absorption of PPy-Cl. The MD-optimized model (Figure S11, Supporting Information) of PPy-Cl reveals an effective water molecules trapping (Figure 3b, inset). Moreover, the pair-correlation function (PCF), i.e. g(r), of H_2O-H_2O pairs, which is an essential means for understanding how molecules interact with each other, is computed to predict the phase of trapped water in the stabilized model.[31] The r value corresponds to the distance between two target molecules (or

atoms), and the g(*r*) value represents the probability of the presence of molecular (or atomic) pairs within specific *r* values.[32] Therefore, the two sharp peaks locating at 1 and 1.5 Å (Figure 3b) represent the O-H and H-H distance, respectively. In another word, the vaporous water can be liquefied by the solvation effect of PPy-Cl, evidencing a different mechanism compared with previously reported AWH.[10]

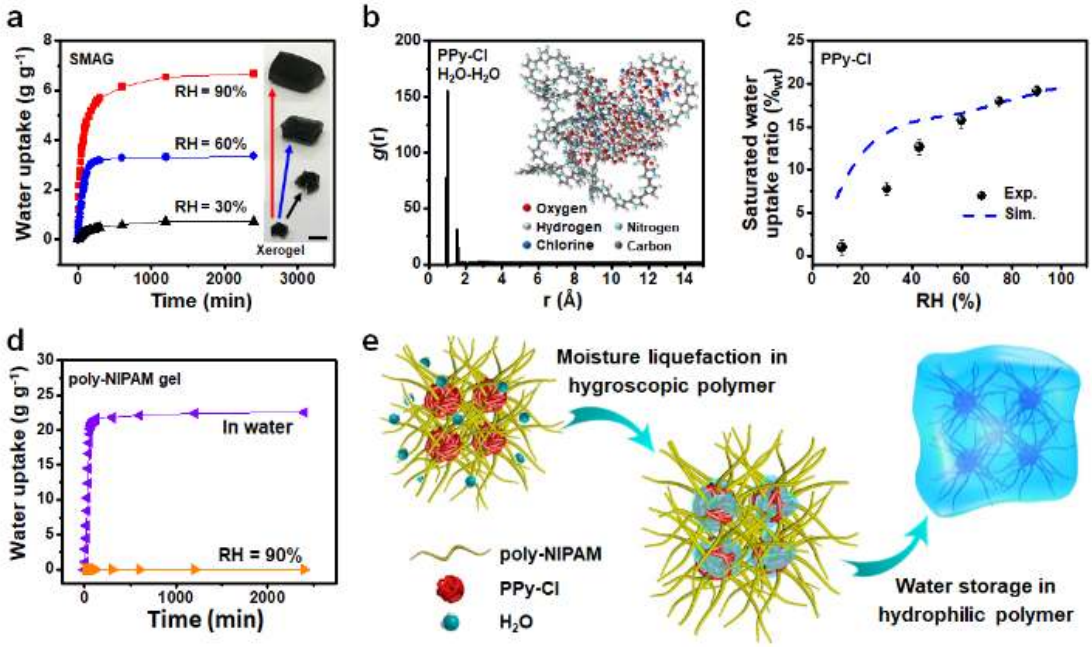

Figure 3. Water capturing with SMAGs. a) The water capturing the behavior of SMAG at RH of 30 %, 60 %, and 90 %; Insets from bottom to top: corresponding dried and hydrated SMAG with equilibrated water uptake (scale bar: 1 cm). b) The pair-correlation function of water molecule pairs from molecular dynamic simulation; Inset: computing model of hydrated PPy-Cl shows the water aggregations in the central part of PPy-Cl clusters. c) The experimental (black points) and simulated (blue dash) data of moisture absorbing based on PPy-Cl at various RH. d), The liquid water (violet curve) and moisture (orange curve) absorption of the poly-NIPAM gel, revealing a superior liquid water absorption and poor moisture capturing of the poly-NIPAM gel. e) Schematic illustration of the moisture absorption enabled by SMAGs.

To further examine the liquefaction-enhanced moisture absorbing of PPy-Cl, the quantitative simulation is performed (Figure 3c, blue dashes). Wherein, the PPy-Cl was equilibrated at different RH, which was simulated by water molecules loaded in the working system at 300 K. The amount of captured water rapidly increases with the rise of RH values when the RH is lower than 40 %, showing a positive correlation between moisture absorption and RH (see Figure S12, Supporting Information, for fugacity dependent water absorbance). The water capacity of PPy-Cl shows a weaker dependence on the RH variation when the RH is higher than 40 %, suggesting an excessive water loading in the simulation system. Moreover, the experiments performed in an RH-controlled container confirm a similar general trend with a slight deviation at low RH region (Figure 3c, black points). Such difference is due to the assumption of ideal contact between water molecules and PPy-Cl chains in the simulation system,[33] while in the experimental condition, it is hardly fulfilled because of the crystalline regions of PPy-Cl at low RH (see Figure S13, Supporting Information). Combining the conclusion so far, we have confirmed that the PPy-Cl component can capture water from the air and liquefied them for storage at various RH.

Despite the efficient moisture absorption of PPy-Cl, its water capacity is still too low to meet the requirement of AWH, especially compared with the aforementioned super water-absorbent gels. The poly-NIPAM can overcome such limitation because of its super-hydrophilicity. As shown in Figure 3d, the poly-NIPAM gel can absorb and store liquid water with a saturated water content of ca. 23 $g\ g^{-1}$. However, only ca. 0.01 g water can be captured from the air by 1 g poly-NIPAM

xerogel, indicating an insufficient water vapor absorption. Therefore, combining such two components to form SMAG can realize efficient moisture absorption and large water capacity simultaneously (Figure S14, Supporting Information). As shown in Figure 3e, the moisture absorption of optimized SMAGs is achieved by two-step water transfer: (1) the water molecules in the air are captured by PPy-Cl; (2) the condensed water is transferred to the poly-NIPAM network for storage (see Figure S15 and S16, Supporting Information, for more the experimental evidence and theoretical analysis).

Another essential feature of the designed SMAG is the rapid water releasing triggered by stimuli-responsive behavior via poly-NIPAM (see *Materials and Methods* for detail). As shown in **Figure 4**a, a typical SMAG, which is highly hydrated by moisture, can directly release ca. 50 % of containing water within 20 min once slightly heated to ca. 40 °C (Figure 4a, red and blue dashes, also see Figure S17 and Supporting Mov. 1, Supporting Information), enhancing the efficiency of water production (blue region in Figure 4a, termed as "express mode" water releasing). After this rapid release of liquid water, the residual water (also see Figure S18, Supporting Information) can be collected via an evaporating-condensing process (orange region of Figure 4a and Figure 4b, termed as "normal mode" water releasing, Figure S19, Supporting Information)[9] with a water releasing rate of ca. 0.3 g g^{-1} h^{-1}. Therefore, the SMAG presents two water releasing modes toward different water content situations, and both can be powered by solar radiation since the PPy-Cl can convert the solar energy to heat. As shown in Figure 4c, the efficient express mode can be attributed to the well investigated thermal-responsive hydrophilicity switching of the poly-NIPAM.[15] When the temperature of the SMAG rises beyond low critical solution temperature

(LCST, also known as hydrophilicity switching temperature)[33] by heating, the hydrophilicity of poly-NIPAM chains is reversed by a conformational change.[34] Thus, the stored water is expelled from the hydrophobic poly-NIPAM network. Since the conformational change is relatively fast (in the order of a minute), the corresponding water release rate is about 10 times faster than that of the normal mode. Also, the amount of residual water is relatively low, which is beneficial to the efficient solar vaporization for water releasing in the normal mode.[35] Compared with previously reported AWH materials that exhibit peak water harvesting rate at certain RH, AWH based on SMAGs covers the broadened working range of RH, which makes it a promising all-weather AWH. Furthermore, the continuous AWH can be achieved by repeating the capturing-releasing cycles. For instance, 1 g of dried SMAG is able to produce ca. 55 g water in 28 h at an RH of ca.75 %, including 28 typical cycles with moisture capturing for 50 min and water releasing for 10 min (Figure S20, Supporting Information).

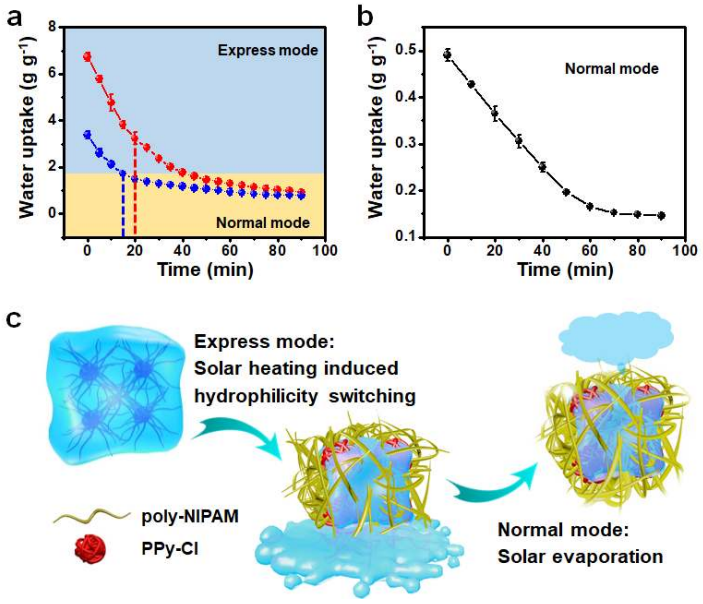

Figure 4. Water releasing with SMAGs. Water releasing modes of SMAGs with a) high and b) low water uptake. The water uptake threshold of the express mode is ca. 1.7 g g^{-1}, showing that the SMAGs can rapidly release large amount of water and steadily produce water from the relatively dry air. c) Schematic illustration of express mode and normal mode for the water releasing powered by solar energy.

The outdoor experiments using natural sunlight further validate the ability of the SMAG to produce water in practical conditions, where factors such as varying environmental humidity and temperature fluctuation often influence the performance. A prototype AWH system based on SMAGs was placed on the roof of Engineering Teaching Center at UT Austin campus. Wherein, the SMAG sample was cut into slices (Figure 5a) and packaged in transparent nylon mesh bags (Figure 5a I and II), which were exposed to air for water capturing, demonstrating a scalable, potentially low-cost design for AWH. The solar vaporized water (i.e. normal mode) was condensed on the transparent condenser (Figure 5a III) and flowed to the bottom, converging with the directly released water upon the express mode (Figure 5a IV). As shown in Figure 5 b and c, upon exposure to the moist air, the original dry SMAG bags display a visible swelling after several hours, indicating that the SMAGs can capture the moisture. The subsequent water releasing of swollen SMAGs was processed by placing the container under natural sunlight.

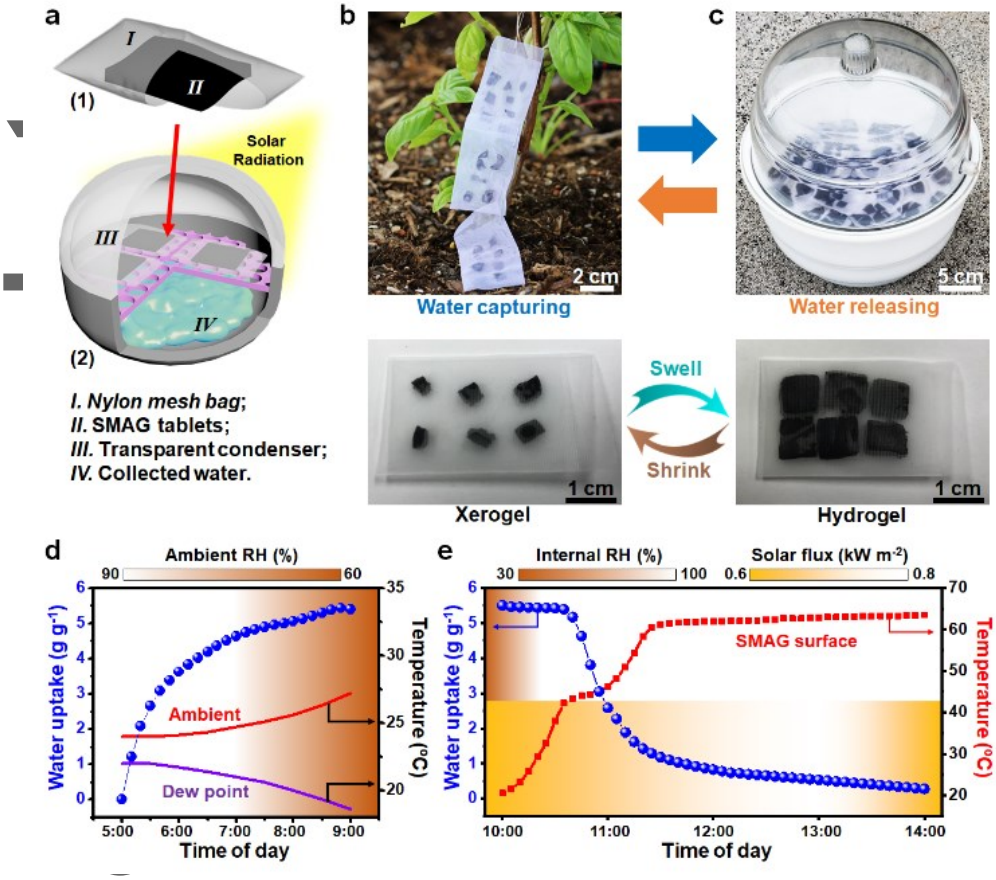

Figure 5. Outdoor AWH powered by natural sunlight. a) Schematic illustration of (1) the water harvester based on SMAGs for (2) the water collector. Photograph of SMAG bags during b) water capturing in the natural environment and c) water releasing under solar radiation. The obvious volume change of SMAGs indicates a large water yield. d) Representative outdoor water capturing process in the early morning (blue curve), where ambient temperature (red curve), dew point temperature (violet curve) and ambient RH (background color map) were presented. e) Representative outdoor water releasing process in noontime (blue curve), where the surficial temperature of SMAG (red curve), internal RH (top background color map) and solar flux (bottom background color map) were presented.

The AWH experiment was carried out from 5:00 a.m. (ca. 1 hour before sunrise) to 9:00 a.m. under a sunshade, where the ambient temperature, RH and dew point temperature were traced

(Figure 5d). In the early morning, the RH was around 85 %, indicating an ideal environment for rapid water harvesting. However, the comparison of ambient temperature (Figure 5d, red curve) and dew point temperature (Figure 5d, violet curve) eliminated the possibility of spontaneous water condensation. Upon exposure to the ambient, the water uptake of SMAG tablets can be increased to 5.4 g g^{-1} in four hours with average water capturing rate of ca. 1.3 g g^{-1} h^{-1} (Figure S21, Supporting Information). Subsequently, the hydrated SMAGs were retrieved and exposed to the sunlight (ca. 0.7 kW m^{-2}) from 10:00 a.m. to 2:00 p.m. (Figure 5e). The water adsorbed at the surface of SMAG tablets can be evaporated by the solar heating, increasing the internal RH of the container (to a saturated state). When the SMAGs was heated to ca. 40 °C, its surface temperature variation was slowed down (Figure 5e red curve), indicating the contained water is releasing in the express mode. The quantitative monitoring of water uptake (Figure 5e blue curve) further confirmed a significant water release of 3.9 g g^{-1} from 10:40 to 11:20. After that, the surface temperature of SMAG gradually increased to ca. 63 °C, which was an equilibrium temperature upon evaporation cooling and solar heating due to the water release in the normal mode. It still contributed to a continuous water release (ca. 0.4 g g^{-1} h^{-1}) after 11:20. The collected water of such a single cycle is about 3.9 g g^{-1}. Compared with the water loss from SMAGs (ca. 4.8 g g^{-1}), the AWH efficiency of our prototype is about 81 %. These results indicate that the SMAGs enable flexible AWH adapting to the natural environment, revealing its potential for practical applications (Figure S22, Supporting Information). Note that the SMAG presented here is designed for the AWH in natural conditions, involving ambient air pressure, humidity and temperature lower than 40 ° C. It should be further improved for particular application in harsh

environments. In addition, the quality of collected water is comparable with distilled water (Figure S23, Supporting Information).

In conclusion, we present here a rationally designed high-efficiency AWH working across a range of RHs via SMAGs that synergistically integrate: (1) hygroscopic PPy-Cl for moisture absorption and liquefaction, (2) hydrophilic network of poly-NIPAM for water storage, and (3) hydrophilicity switching based on the poly-NIPAM for rapid water release. These synergistic functions are enabled by effective water transport along the interpenetrating networks of functional polymers. Apart from the demonstrated AWH, this design represents a promising strategy for developing atmospheric water management with high-capacity storage, controllable phase transformation, and tunable water transport through polymeric networks. Furthermore, this strategy provides insight into the synergetic effect of interpenetrated functional polymers and their potential for advanced AWH systems in the future.

Supporting Information

Supporting Information is available from the Wiley Online Library or from the author.

Acknowledgments

F. Z. and X. Z. contributed equally to this work. G.Y. acknowledges the financial support from the Sloan Research Fellowship, Camille-Dreyfus Teacher-Scholar Award, and the National Science Foundation award (NSF-CMMI-1537894).

Received: ((will be filled in by the editorial staff))
Revised: ((will be filled in by the editorial staff))
Published online: ((will be filled in by the editorial staff))

References

[1] Core Writing Team, R. K. Pachauri, L. Meyer, *Climate Change 2014: Synthesis Report.* (IPCC, Geneva, Switzerland, **2014**).

[2] A. Deepak, T. D. Wilkerson, L. H. Ruhnke, Eds., *Atmospheric Water Vapor*. (Elsevier, **2013**).

[3] A. R. Parker, C. R. Lawrence, *Nature*, **2001** *414*, 33.

[4] Y. Zheng, H. Bai, Z. Huang, X. Tian, F.-Q. Nie, Y. Zhao, J. Zhai and L. Jiang, *Nature,* **2010**, *463*, 640.

[5] Z. Pan, W. G. Pitt, Y. Zhang, N. Wu, Y. Tao and T. T. Truscott, *Nature Plants.*, **2016**, *2*, 16076.

[6] J. Ju, H. Bai, Y. Zheng, T. Zhao, R. Fang and L. Jiang, *Nature Commun.*, **2012**, *3*, 1247.

[7] K. C. Park, P. Kim, A. Grinthal, N. He, D. Fox, J. C. Weaver and J. Aizenberg, *Nature*, **2016**, *531*, 78.

[8] N. Miljkovic, R. Enright, Y. Nam, K. Lopez, N. Dou, J. Sack and E. N. Wang, *Nano*

Lett., **2013**, *13*, 179.

[9] P. Gandhidasan and H. I. Abualhamayel, *Water. Environ. J.*, **2007**, *21*, 19.

[10] H. Kim, S. Yang, S. R. Rao, S. Narayanan, E. A. Kapustin, H. Furukawa, A. S. Umans, O. M. Yaghi and E. N. Wang, *Science*, **2017**, *356*, 430.

[11] A. Lee, M.-W. Moon, H. Lim, W.-D. Kim and H.-Y. Kim, *Langmuir*, **2012**, *28*, 10183.

[12] C. T. Kresge and W. J. Roth, *Chem. Soc. Rev.*, **2013**, *42*, 3663.

[13] D. A. Loy and K. J. Shea, *Chem. Rev.*, **1995**, *95*, 1431.

[14] L. Yu, K. Dean and L. Li, *Prog. Polym. Sci.*, **2006**, *31*, 576.

[15] R. Li, Y. Shi, L. Shi, M. Alsaedi, P. Wang. *Environ. Sci. Technol.* **2018***, 52,* 5398.

[16] Y. Tu, R. Wang, Y. Zhang, J. Wang. *Joule*, **2018**, *2*,1452.

[17] T. Ono, T. Sugimoto, S. Shinkai and K. Sada, *Nat. Mater.*, **2007**, *6*, 429.

[18] Y. Yang, D. Rana and C. Q. Lan, *RSC Adv.*, **2015**, *5*, 59583-59590.

[19] E. W. Jager, E. Smela and O. Inganäs, *Science*, **2000**, *290*, 1540-1545.

[20] G. G. Wallace, P. R. Teasdale, G. M. Spinks and L. A. Kane-Maguire, *Conductive Electroactive Polymers: Intelligent Polymer Systems*. (Boca Raton: CRC press, **2008**).

[21] L. Pan, A. Chortos, G. Yu, Y. Wang, S. Isaacson, R. Allen, Y. Shi, R. Dauskardt and Z. Bao, *Nature Commun.*, **2014**, *5*, 3002.

[22] Y. Shi, L. Peng, Y. Ding, Y. Zhao and G. Yu, *Chem. Soc. Rev.*, **2015**, *44*, 6684-6696.

[23] Y. Wang, Y. Shi, L. Pan, Y. Ding, Y. Zhao, Y. Li, Y. Shi and G. Yu, *Nano Lett.*, **2015**, *15*, 7736-7741.

[24] M. Hasik, A. Bernasik, A. Drelinkiewica, K. Kowalski, E. Wenda and J. Camre, *Surf.*

Sci., **2002**, *507*, 916-921.

[25] J. Tabačiarová, M. Mičušík, P. Fedorko and M. Omastová, *Polym. Degrad. Stabil.*, **2015**, *120*, 392-401.

[26] H. Furukawa, F. Gańdara, Y.-B. Zhang, J. Jiang, W. L. Queen, M. R. Hudson and O. M. Yaghi, *J. Am. Chem. Soc.*, **2014**, *136*, 4369–4381.

[27] J. Canivet, A. Fateeva, Y. Guo, B. Coasne and D. Farrusseng, *Chem. Soc. Rev.*, **2014**, *43*, 5594–5617.

[28] N. C. Burtch, H, Jasuja and K. S. Walton, *Chem. Rev.*, **2014**, *114*, 10575–10612.

[29] C. Wang, X. Liu, N. K. Demir, J. P. Chen and K. Li, *Chem. Soc. Rev.*, **2016**, *45*, 5107–5134.

[30] S. Anand, A. T. Paxson, R. Dhiman, J. D. Smith and K. K. Varanasi, *ACS Nano.*, **2012**, *6*, 10122–10129.

[31] M. M. Ostwal, M. Sahimi and T. T. Tsotsis, *Phys. Rev. E.*, **2009**, *79*, 061801.

[32] X. P. Chen, Q. H. Liang, J. K. Jiang, Cell K. Y. Wong, Stanley Y. Y. Leung, H. Y. Ye, D. G. Yang and T. L. Ren, *Sci. Rep.*, **2016**, *6*, 20621.

[33] J. T. Zhang, S. X. Cheng and R. X. Zhuo, *Colloid. Polym. Sci.*, **2003**, *281*, 580-583.

[34] B. Sun, Y. Lin, P. Wu and H. W. Siesler, *Macromolecules,* **2008**, *41*, 1512-1520.

[35] G. Ni, G. Li, Svetlana V. Boriskina, H. Li, W. Yang, T. J. Zhang and G. Chen, *Nat. Energy.*, **2016**, *1*, 16126.

TABLE OF CONTENTS

Super Moisture-Absorbent Gels that consist of functional polymers simultaneously exhibit hygroscopicity and controllable hydrophilicity. Such a gel can spontaneously capture atmospheric water, and efficiently deliver liquid water under various environmental conditions. This work not only reveals the essential of gel-based moisture absorbency, but also paves the way for the fresh water production from the air.

Keyword: hydrogel, polymer, solar energy, moisture absorbing, water production